ADVANCED FUNCTIONAL MATERIALS
www.afm-journal.de

Light-Driven Titanium-Dioxide-Based Reversible Microfireworks and Micromotor/Micropump Systems

By *Yiying Hong, Misael Diaz, Ubaldo M. Córdova-Figueroa,** and *Ayusman Sen**

Titanium dioxide (TiO_2) possesses high photocatalytic activity, which can be utilized to power the autonomous motion of microscale objects. This paper presents the first examples of TiO_2 micromotors and micropumps. UV-induced TiO_2 reversible microfireworks phenomenon was observed and diffusiophoresis has been proposed as a possible mechanism.

1. Introduction

The past 5 years witnessed the development of the first generation of catalytic motors on the micro-/nanoscale.[1] These are the initial attempts at designing self-propelled motors with the intention of further scaling down to the molecular scale. The significant viscous drag in the low Reynolds number regime[2,3] and the increased dominance of Brownian motion at small scale forced us to seek unconventional routes in powering the micro/nano-objects.[4,5] Most systems up to now are bubble propulsion motors[6–8] and self-electrophoretic motors that involve bimetallic nanowires[9–12] or enzyme-functionalized carbon fibers,[13] in addition to a few newly developed photo-induced self-diffusiophoretic motors.[14–17] These motor systems often involve toxic chemicals (H_2O_2, N_2H_4, HCl) that are not appropriate for in vivo applications, or produce bubbles that limit the use. Herein we present a novel and versatile catalytic micromotor system, which is the cleanest and simplest of its kind. We use titanium dioxide (TiO_2) to convert optical energy to mechanical energy via photocatalysis. The whole system consists only of titania, water, sometimes organics, and light input. The system is very forgiving, requiring no careful control of substrate concentration or catalyst conditioning, and is easily controllable by external light.

[*] Prof. U. M. Córdova-Figueroa, M. Diaz
Department of Chemical Engineering
University of Puerto Rico-Mayagüez
Box 9000, Mayaguez, PR 00681-9000 (USA)
E-mail: ubaldom.cordova@upr.edu
Prof. A. Sen, Y. Hong
Department of Chemistry
Pennsylvania State University
University Park, PA 16802 (USA)
E-mail: asen@psu.edu

DOI: 10.1002/adfm.201000063

2. Results

The photoactivity of TiO_2 comes from its hole–electron separation triggered by photons of energy equal to or higher than its bandgap (Eq. 1).[18–21]

$$TiO_2 \xrightarrow{h\nu} TiO_2\ (h^+ + e^-) \begin{cases} \xrightarrow{O_2} \cdot O_2^- \\ \xrightarrow{H_2O} \cdot OH + H^+ \end{cases} \quad (1)$$

A large fraction of the polarons[22] recombine while a small fraction migrate to the surface and react with available redox species.[23] Usually the polarons react with water or oxygen to induce complex radical chain reactions.[18] Among the products are superoxide ($\cdot O_2^-$) and hydroxyl radicals ($\cdot OH$), which are highly oxidative and can decompose organic compounds. TiO_2 has been used for water treatment and other decontamination purposes because of its photoactivity.[18,19,24] The reactions produce more product molecules than the reactants consumed, making it possible to propel a TiO_2 particle by the mechanism of osmotic propulsion[5] or diffusiophoresis.[15,25] However, as we found out, the presence of an organic substrate was not necessary for the movement that we observe with TiO_2. Typically, the experiments were done on a sodium borosilicate glass slide in deionized water with no solute added.

There are two categories of autonomous movement associated with TiO_2 that we will discuss in this paper: i) the photo-induced motility of micro-TiO_2 particles and ii) the photo-induced reversible microfireworks.

2.1. Self-Propelled Motion

The motility test was done with commercially available anatase TiO_2 particles (size range 0.2–2.5 μm). They were co-dispersed with nonreactive silica particles (SiO_2, 2.34 μm) at a density of about $7 \times 10^9\ m^{-3}$, which served as tracer particles, and subjected to ultraviolet light (UV) irradiation at 365 nm (center, 2.5 W cm^{-2}). The TiO_2 particles moved at $10 \pm 3\ \mu m\ s^{-1}$ upon UV exposure, and the movement stopped immediately after the UV source was removed (Video 1 of Supporting Information). The UV-induced movement of bigger TiO_2 particles was also observed but at much lower speeds as large colloidal particles experience stronger drag

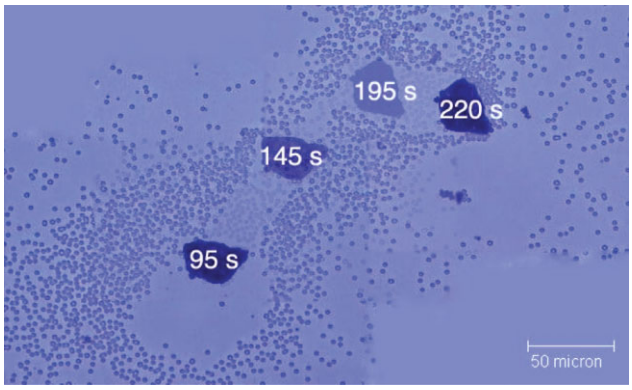

Figure 1. A TiO_2 boat moves under UV as it cuts through the crowd of SiO_2 particles. The picture was edited in Adobe Photoshop by merging four individual photos and the blank space at the corners was filled up with the background color.

force in the low Reynolds number regime. Figure 1 shows a micrometer-sized TiO_2 boat advancing under UV illumination as it cuts through the crowd of SiO_2 particles. Occasionally, due to the asymmetric arrangement of different segments within a particle, we have TiO_2 rotors (Video 2 of Supporting Information).

2.2. Microfireworks

The SiO_2 particles have a strong tendency to gather around TiO_2 particles. This aggregation happens before UV exposure, and is not a result of ambient light or microscope halogen light, as was confirmed by experiments in a dark room. The TiO_2 particles can be either negative or positive (ζ-potential was measured to be -50 to $+26$ mV), depending on the synthesis conditions and the bathing solution. Regardless of the charge, attractive interactions between TiO_2 and other colloidal particles were always observed. Both negatively charged SiO_2 (-70 to -30 mV, $d = 2.34$ μm) and positively charged amidine polystyrene (amidine-PS) particles ($+40$ to $+70$ mV, $d = 2.5$ μm) aggregated around TiO_2. When the SiO_2 particles are coated with 60–80 nm TiO_2 on a hemisphere, the whole Janus particle exhibits varying ζ-potentials (-107 to 20 mV). They aggregate spontaneously as well (Fig. 2). Notice that in the presence of silica, the aggregation is usually in a close-packed manner, whereas the aggregation involving TiO_2 and amidine-PS is looser.

Upon the exposure to UV light, the neighboring colloidal particles immediately move away from the TiO_2 particle in the center, whether they are negative or positive. Nearby TiO_2 particles move away from each other as well. This creates an exclusion zone cleared of particles around each individual TiO_2 particle (see Fig. 1). When the UV source is removed, the tracer particles pull back toward the TiO_2 particle and form the aggregates again. This process is not a mere relaxation, for it shows strong directionality (toward the TiO_2 center), and it proceeds at a much faster rate than Brownian relaxation, though more slowly than the expansion process (Supporting Information Fig. S14). Janus particles that contain both SiO_2 and TiO_2 segments also move away from each other; a phenomenon that is reversible (Fig. 3). The behavior of the SiO_2–TiO_2 Janus particles is consistent with what was observed for systems consisting of pure TiO_2 and SiO_2 particles. The expansion–contraction process is repeatable as can be seen from Figure 4, however, with a decaying trend with the expansion size getting progressively smaller. From Figure 4, we also see that the expansion is faster than the contraction. Figure 5 shows that SiO_2 particles move away from TiO_2 much more quickly than do amidine-PS particles. It should be noted that extended exposure to UV light results in aggregation of TiO_2 particles of 1–10 μm-size inside the UV spot. TiO_2 absorbs UV energy and exhibits positive phototactic response. Using this property, we were able to use UV light to migrate a group of SiO_2–TiO_2 Janus particles (Video 3 of Supporting Information). SiO_2 particles also re-aggregate around TiO_2 particles upon long-term exposure to UV light, which may be a result of thermal gradients (Supporting Information Fig. S15). However, this long-term phenomenon is beyond the scope of the paper and will not be discussed in more detail. The phenomena observed at short times are unlikely to be due to thermal effect, especially considering the fast response times and the high thermal capacity of water.

The size of the expansion, L, measured as the distance from the edge of the exclusion zone to the edge of the central TiO_2 particle, is sensitive to the size of the TiO_2 particle. Larger TiO_2 particles repel more strongly. TiO_2 particles smaller than 1–2 μm usually do not repel at all. This expansion size/TiO_2 particle size relationship is depicted in Figure 6. Large variations are seen in the graph because the activity of TiO_2 is very sensitive to its crystallinity, number of defect sites, and surface conditions. No special attention was paid in controlling the uniformity of our TiO_2 particles; thus variation in activity was expected. The positive amidine-PS particles also move away from TiO_2 particles upon UV exposure, but only give a clear exclusion zone after longer exposure (5–10 min).

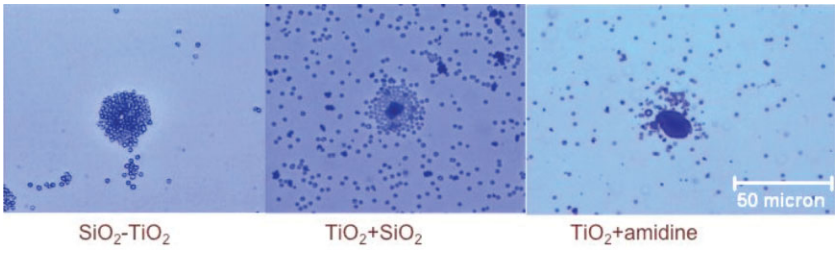

Figure 2. The spontaneous aggregation observed with SiO_2–TiO_2 Janus particles (left), between TiO_2 and SiO_2 particles (middle), and between TiO_2 and amidine particles (right) in the absence of UV light.

2.3. Micropumps

By Galilean inverse, a micromotor fixed to a surface should act as a microfluidic pump. Figure 7 shows different designs of TiO_2 thin film (80 nm) pumps on a glass surface. The TiO_2 film is capable of driving the fluid in the direction away from it. One interesting design is a ring-shaped TiO_2 film. While the ring pushes most particles out, the particles that are trapped within the inner circle are packed in (Fig. 7 bottom). Our TiO_2 system provides an

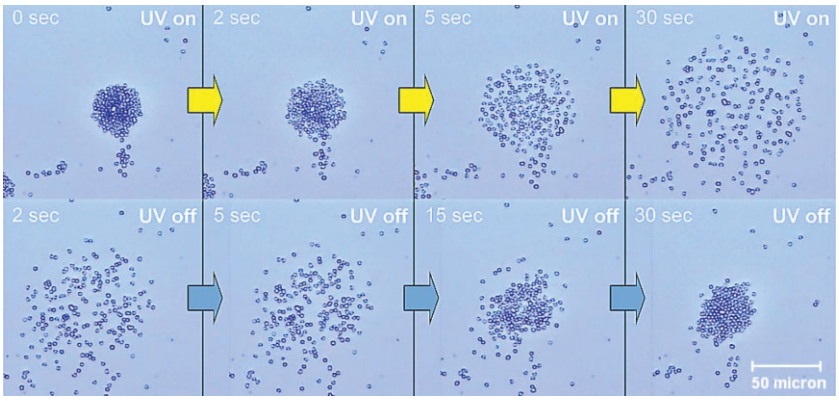

Figure 3. The SiO_2–TiO_2 Janus particles in deionized water aggregated in the absence of UV and repelled each other when UV is switched on. The process is reversible.

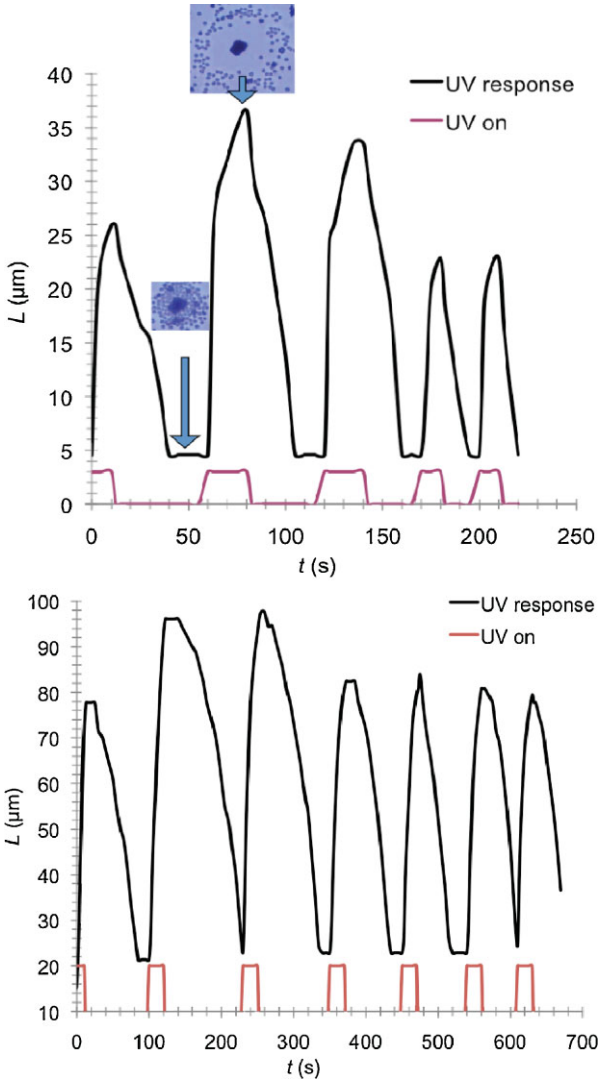

Figure 4. Cycles of expansion–contraction between TiO_2 particle and SiO_2 particles. The *y*-axis, *L*, represents the diameter of the expanded circle. The substrate was deionized water (top) and 5% v/v methanol in water (bottom).

eazy, clean, and controllable way of directing fluid in microfluidic devices.

3. Discussion

3.1. Diffusiophoretic Model

We examined the possibility of a diffusiophoresis mechanism for the observed movements. Electrolyte diffusiophoresis[26] is caused by differential diffusion of ions, which sets up a temprorary electric field and chemical pressure field that drive a charged particle to move. A simple test of the theory is to add electrolytes to the solution. From Smoluchowski equation $U = \frac{\varepsilon\zeta E_0}{\eta}$ for large κa (κ^{-1}: Debye length, a: diameter) sphere, we know that in a medium of ε dielectric constant and η viscosity, a spherical particle moves at velocity U under an electric field E_0. If the ζ-potential decreases to near zero, the velocity U approches zero too. The ζ-potential can be reduced by the addition of electrolytes. With 0.5 mM of hydrochloric acid (HCl), sodium chloride (NaCl), or sodium hydroxide (NaOH), the outward "fireworks" were completely quenched. This is consistent with the diffusiophoresis hypothesis.

In a diffusiophoretic model, the locomotion may be caused by the diffusion of chemical species photogenerated by TiO_2 ($\cdot O_2^-$, $\cdot OH$, H^+, OH^-, etc.). The diffusiophoretic mechanism is illustrated in Figure 8. The surface of the particle produces ionic products that diffuse at different speeds. As a result, a temporary electric field is built up around the particle, which can drive charged tracer particles to move in a direction depending on their ζ-potential. Meanwhile, the overall electrolyte concentration is higher near the center. This causes a chemophoretic flow in the direction of lower electrolyte concentration driven by the chemical

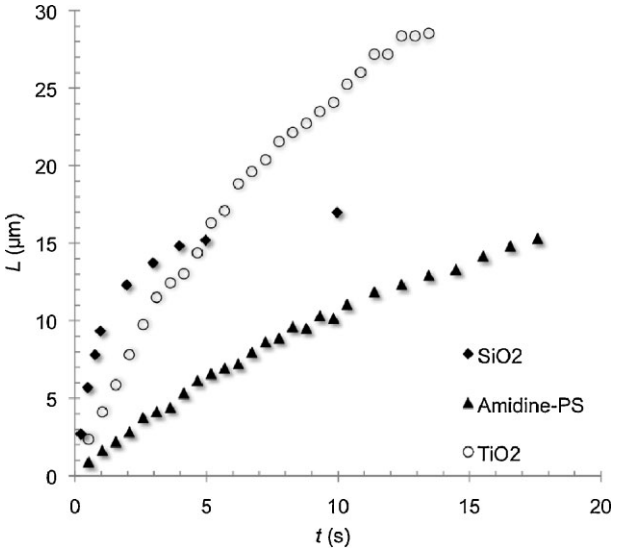

Figure 5. The average distance of the tracer particles from the TiO_2 particle increases over time upon UV exposure.

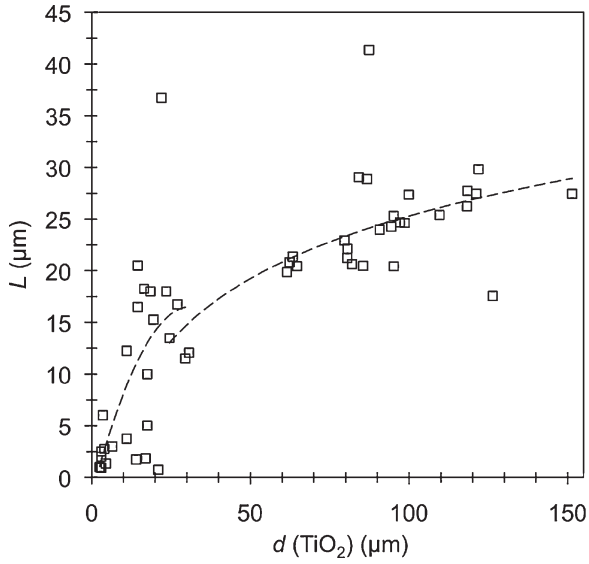

Figure 6. The size of expansion increases with the size of TiO_2 particle. The diameter, $d(TiO_2)$, was approximated by averaging the long axis and short axis of an irregularly shaped particle. Tracer particles are SiO_2.

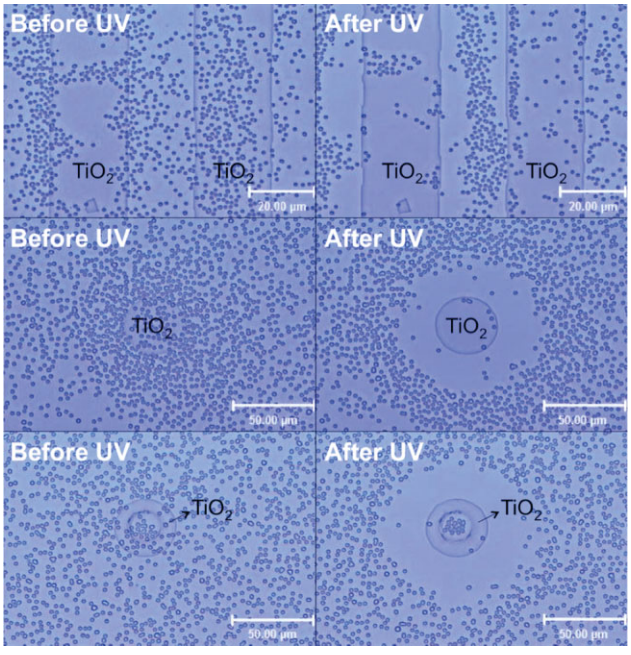

Figure 7. Various designs of TiO_2 surface pumps.

pressure. In combination, the diffusiophoresis velocity is given by[26]

$$U = \frac{\varepsilon}{4\pi\eta}\frac{kT}{eZ}\left[\beta\zeta - 2\frac{kT}{eZ}\ln(1-\gamma^2)\right]\nabla \ln C_\infty \quad (2)$$

where U is the velocity of the particle, ε the permitivity, η the viscosity of the solution, kT the thermal energy, e the elementary charge, Z the charge of the ion, ζ the "effective" ζ-potential,

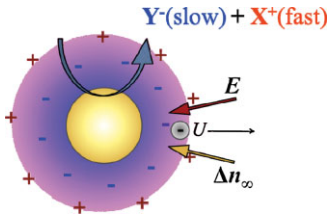

Figure 8. Electrolyte diffusiophoresis caused by reaction on a particle surface. X^+ and Y^- are the ionic products, which diffuse at different speeds. E is the electric field built up by the differential diffusion of the ionic products. The overall electrolyte concentration n decreases from the particle surface. As a result, a negative tracer particle moves at velocity U along the direction pointed by the solid black arrow due to both electrophoresis and chemophoresis.

$\gamma = \tanh(eZ\zeta/2kT)$, and $\nabla \ln C_\infty$ is the local concentration gradient.

To obtain a prediction of the velocity while the UV light is on and to account for the curvature effect, we solve the diffusion equation in spherical coordinates:

$$\frac{\partial c}{\partial t} = D\frac{1}{r^2}\frac{\partial}{\partial r}\left(r^2\frac{\partial c}{\partial r}\right) \quad (3)$$

where t is the time, r the radial dimension, D the diffusion coefficient of product species, and c is the charged species concentration. To model diffusion during the fireworks response, we assume a constant flux j_0 of product ions at the surface of TiO_2. For simplicity, we neglect any ionic charge effects to their diffusion. Also, it is assumed that the concentration far from the TiO_2 particle is zero, as given by the boundary conditions:

$$-D\frac{\partial c}{\partial r} = j_0 \text{ at } r = b \quad (4)$$

$$c \to 0 \text{ as } r \to \infty$$

where b is the radius of the TiO_2 particle. Moreover, only a negligible concentration of charged species is assumed to exist before turning on the UV light:

$$c(r, t=0) = 0 \quad (5)$$

For convenience, we adimensionalize Equation 3:

$$\frac{\partial c}{\partial \tau} = \frac{1}{\bar{r}^2}\frac{\partial}{\partial \bar{r}}\left(\bar{r}^2\frac{\partial c}{\partial \bar{r}}\right) \quad (6)$$

In Equation 6, $\tau = t/(b^2/D)$ and $\bar{r} = r/b$. A solution to Equation 6 subject to the corresponding boundary conditions can be found by the Laplace transform method:

$$c(\bar{r}, \tau) = \frac{j_0 b}{D} \times \frac{1}{\bar{r}}\left[\operatorname{erfc}\left(\frac{\bar{r}-1}{2\sqrt{\tau}}\right) - \exp(\tau)\exp(\bar{r}-1)\operatorname{erfc}\left(\sqrt{\tau}+\frac{\bar{r}-1}{2\sqrt{\tau}}\right)\right] \quad (7)$$

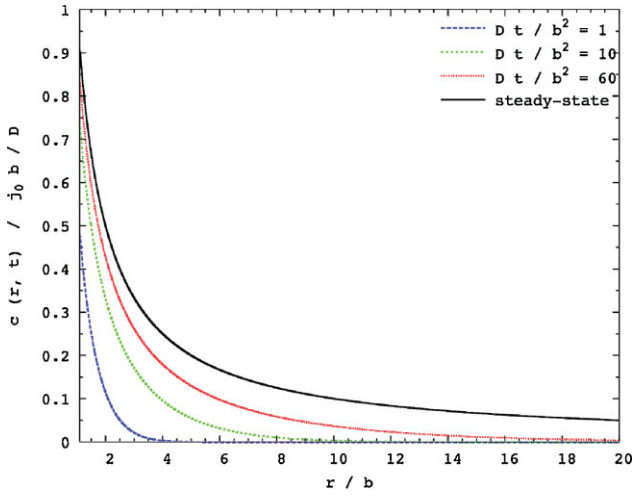

Figure 9. Concentration profile as a function of time and position.

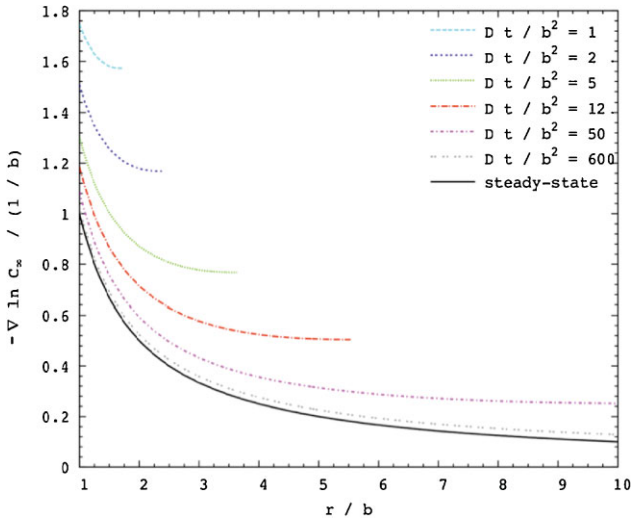

Figure 10. Gradient as a function of the distance from a TiO_2 particle at any time.

The value $j_0\, b/D$ represents the characteristic concentration of product ions on the surface of the TiO_2 particle. Note from Figure 9 that the charged species diffuse from the surface of TiO_2, and as time increases these species move farther away from the surface until they reach a steady concentration profile, given by

$$c(\bar{r}) = \frac{j_0 b}{D}\frac{1}{\bar{r}} \tag{8}$$

Considering that the fireworks response involves multiple particles, estimation of the local chemical gradient also depends on the particle concentration since they slow down the diffusion of the charged species. For simplicity, we neglect any disturbances caused by the presence of the particles, as if they were far from each other. We have computed the concentration gradient in Equation 2 by considering that $\nabla \ln C_\infty = \frac{1}{C_\infty}\frac{\partial C_\infty}{\partial \bar{r}}$ and approximating it by the concentration gradient developed by the charged species produced on the TiO_2 surface. By differentiation and subsequent division of Equation 7, we obtain

$$\nabla \ln C_\infty = 1 - \frac{1}{r} + 1 \Bigg/ \left(-1 + \frac{e^{(-1+r+\tau)}\,\mathrm{erfc}\left(\frac{-1+r+2\tau}{2\sqrt{\tau}}\right)}{\mathrm{erfc}\left(\frac{-1+r}{2\sqrt{\tau}}\right)} \right) \tag{9}$$

Similar to the concentration profile given in Figure 9, Figure 10 shows that the ions propagate from the surface of TiO_2 until the concentration gradient reaches a steady-state profile. The tracer particles move in the concentration gradient until the gradient drops below a certain number. From Figure 10 we notice that given the same concentration gradient cut-off (y-axis), the smaller the TiO_2 particle is (larger Dt/b^2), the shorter is the travel distance (r/b), consistent with the trend observed in Figure 6. Other factors, such as flux j_0 dependence on particle size and particle concentration, are not necessarily eliminated as possible contributors. We have studied analytically only one single species and its diffusive behavior. Other charged species are produced during UV exposure that could alter the total concentration profile, and consequently cause other significant additions to the concentration gradient—the "driving" force—leading from a mass conservation perspective to a description of the behavior in Figure 6.

We use Equation 9 to estimate the gradient and consequently, the velocity of any particle as a function of time and position. The constants and parameters for the calculation are listed in Supporting Information Table S1. The diffusivities of the product species suggests that $\beta \approx 1$; thus we use $\beta = 1$ in our calculations.

To calculate the theoretical velocity, we assume that the gradient of charged species at any distance from the TiO_2 particle is equal to the steady state gradient, as shown in Figure 10. In less than 1.5 s after turning on the UV light, we obtain a dimensionless diffusive time Dt/b^2 of about 700, meaning that the gradient achieves equilibrium very quickly in comparison to the time that the surrounding particles experience directed motion. Figure 11 shows the experimental and theoretical velocity for negative silica and positive amidine-PS particles as the distance from the surface of TiO_2 is increased. Two glass wall ζ-potentials (-60 mV[27] and -30 mV[28]) are taken into account to show the influence of glass ζ-potential on the movement. The experimental velocity of silica particles decays much more quickly than the theoretical velocity. This is most likely due to the fact that the high density of silica particles is slowing down the diffusion of chemicals. The predicted speed for silica particles is also lower than that observed. It is possible the concentration gradient is underestimated since we assumed a steady state concentration profile. Further, we believe that the diffusion of charged species is not solely responsible for the fireworks phenomenon. Neutral molecule diffusiophoresis can also cause particle movements and, in addition, imbalance in solute density on the two sides of the particle may drive osmotic propulsion.[5]

The prediction for amidine-PS particles does not agree with the experimental observation. A few factors might have caused this disagreement: i) the photoreaction products could change the local chemical environment, which results in the change of ζ-potential upon UV irradiation. The surface of amidine-PS particle is

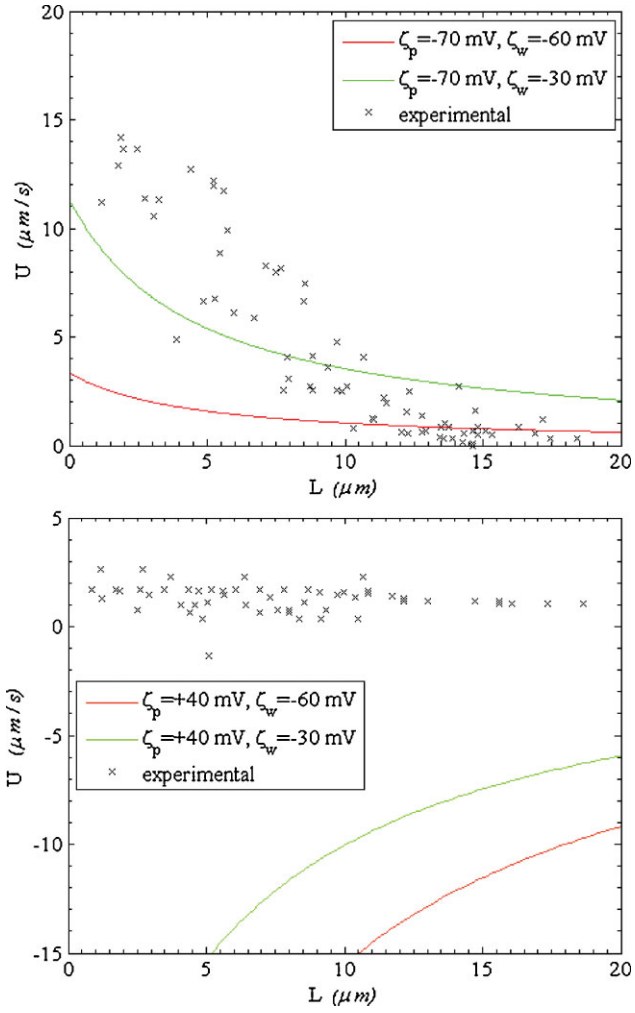

Figure 11. Comparison of the experimental and theoretical velocity of silica (top) and amidine-PS (bottom) particles.

composed of =NH and $-NH_2$ groups which are much more reactive than the oxide/hydroxide groups on silica. Thus, the ζ-potential of amidine-PS is more easily changed under an oxidative environment. ii) Osmotic propulsion in the outward direction offsets the diffusiophoresis effect of a positive particle. In the case of negatively charged silica, the osmotic propulsion and diffusiophoresis both point toward the lower concentration region, whereas in the case of positively charged amidine-PS, diffusiophoresis predicts movement toward the higher concentration region while osmotic propulsion is not affected by the charge of the particle. Therefore amidine-PS particles move away from TiO_2 but more slowly than silica particles do (Fig. 5). As discussed below, under modified experimental conditions, the direction of motion of amidine-PS particles, based on diffusiophoretic mechanism, and electrostatic interactions, becomes more predictable.

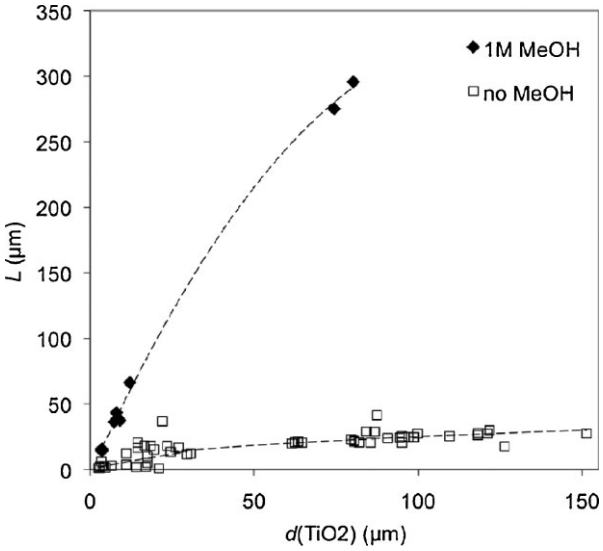

Figure 12. The expansion size as a function of TiO_2 particle size in deionized water and 5% v/v methanol (MeOH). Tracer particles are SiO_2.

3.2. Alcohols Promote the Fireworks Response

We have used methanol as a hole scavenger to promote the photoreaction. A hole scavenger reacts with the photo-induced holes (Eq. 10), making the bottom level of the conduction band more negative to facilitate the reduction reaction.[29] The more reactive electrons therefore combine with available protons in the solvent and hydrogen (H_2) is usually produced

$$TiO_2(h^+ + e^-) + RCH_2OH \rightarrow TiO_2(e^-) + R\dot{C}HOH + H^+ \quad (10)$$

In our experiments, we observed a significant increase in the expansion size (Figs. 12 and 13) and higher reversibility with 5% v/v methanol as the substrate (Fig. 4 bottom). The production of H_2 was confirmed by gas chromatography (Supporting Information Fig. S13). No detectable amount of oxygen or hydrogen was produced during the UV exposure without alcohol (Supporting Information Fig. S12). It is possible that the production of more radical species or H_2, or a combination of the two factors

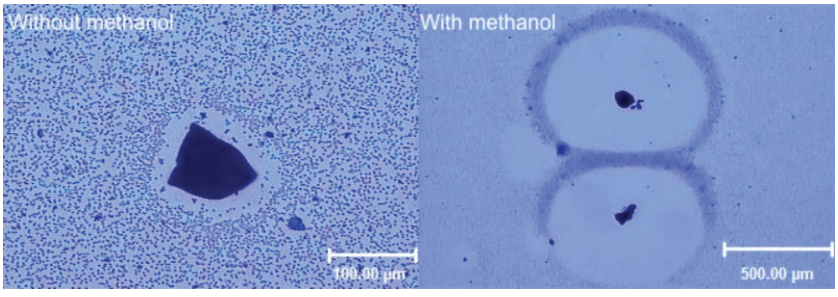

Figure 13. The effect of 10% methanol in enhancing the repelling power of TiO_2. Pictures show the maximum expansion with similarly sized TiO_2 particles without (left) and with (right) methanol.

Table 1. The effect of TEMPO concentration on the UV-induced particle interaction between TiO_2 and SiO_2.

Concentration of TEMPO	Observations
1 mM	Before UV: some aggregations After UV: outward movement
100 mM	Before UV: some light aggregations After UV: almost no response; occasional outward movement
1 M	Before UV: no aggregation After UV: strong inward movement close to TiO_2 particles; moderate outward movement farther away
>>1 M	Before UV: no aggregation After UV: strong inward movement; no outward movement

contributes to the stronger repulsion power because of the osmotic propulsion mechanism.

3.3. Radical Trap Reverses the Fireworks Response

We also used a radical trap, 2,2,6,6-tetramethylpiperidine-1-oxyl (TEMPO), to test the involvement of radicals in the fireworks motions. We predicted that as TEMPO captures the radicals, the radical concentration profile will be weakened or even reversed. The observations are summarized in Table 1. As the concentration of TEMPO increases, the outward motion of SiO_2 tracers becomes weaker and at 1 M, strong inward motion was observed in the close vicinity of TiO_2 while outward motion was still observed farther away. At concentrations much higher than 1 M, no outward motion was observed at all. Layers of tightly packed SiO_2 particles form around the TiO_2, which loosen up when the UV light is removed (Fig. 14). The accelerating motion of SiO_2 particles toward a nearby TiO_2 particle is illustrated in Figure 15.

It is notable that at 1 M TEMPO concentration, strong inward motion near the TiO_2 particle and outward motion farther away from the TiO_2 were observed simultaneously. This suggests the possibility of multiple mechanisms working together. The phenomenon we observed with TEMPO might be a result of charge interaction as well. TEMPO can serve as an electron scavenger, which by combining with the electron polarons, leaves behind positive charge on TiO_2. This was confirmed by using amidine-PS as the tracer particle, where particles continue to move out at 1 M TEMPO concentration, whereas silica particles move toward the TiO_2 instead. The positive charge attracts nearby SiO_2 particles, whereas phoretic flows from chemical diffusion works at longer range and keeps driving more distant particles away.

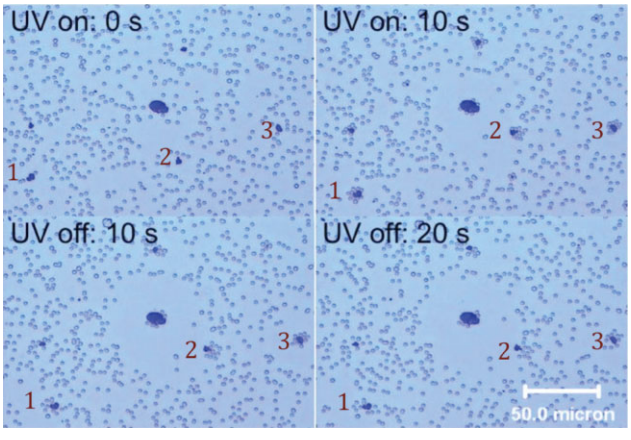

Figure 14. The effect of 1 M TEMPO in altering the "firework" behavior between the TiO_2 and SiO_2 particles. Notice the particles next to the numbers. Attractive motions occur after the UV switches on, and the tightly packed particles loosen after the UV is removed.

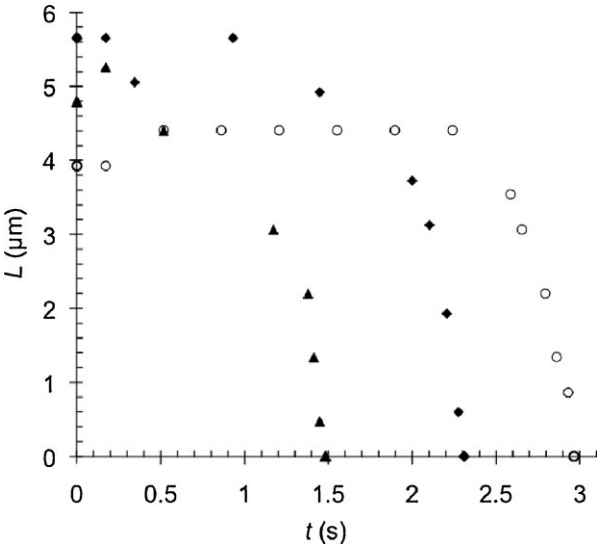

Figure 15. The distance of individual SiO_2 particles from the TiO_2 particle decreases over time as the SiO_2 particles move toward the TiO_2 particle in the presence of 1 M TEMPO in water under UV light.

In general, the electrostactic interaction between TiO_2 and the tracers is enhanced by adding either a hole or an electron scavenger which, respectively, enhances either the negative or positive charge on the TiO_2 particle. Thus, methanol combines with TiO_2 surface holes and increases surface negativity. The TiO_2 repels negative SiO_2 particles much farther while inducing more contractive motions with positive amidine PS particles. On the other hand, TEMPO combines with TiO_2 surface electrons and increases surface positivity. Above certain TEMPO concentrations, the TiO_2 attracts negative SiO_2 particles while it continues to repel positive amidine-PS particles.

3.4. TiO_2 Surface Analysis

There is a possibility that residual organics from the synthesis process, particularly the surfactants, on the surface of TiO_2 particles might be responsible for the fireworks activity as they may provide small amounts of decomposition products which can cause diffusiophoresis. This was shown to be unlikely by three pieces of evidence: i) we do not see a significant difference in the expansion size as we continue to wash off the surface residues. Figure 16 shows that as the solution conductance decreases, the expansion size remains at about the same level. ii) TiO_2 from

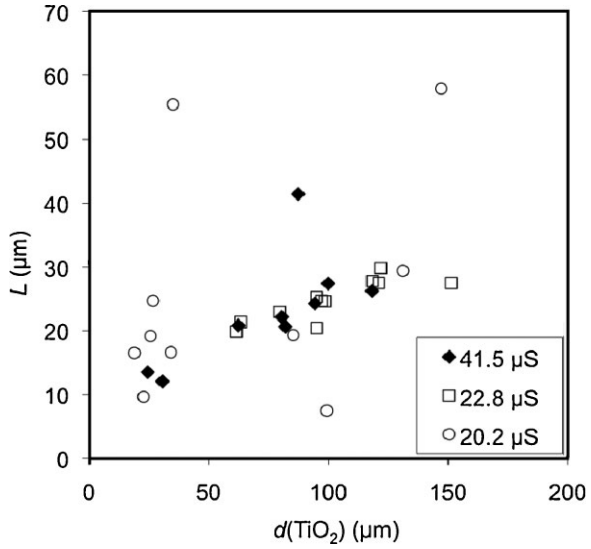

Figure 16. The expansion size as a function of TiO_2 diameter. The TiO_2 particles were washed repeatedly to remove residual surfactants on the surface. The degree of remaining surfactants is indicated by the conductance of the solution (inset).

chemical vapor deposition (where organic contamination is unlikely) in the form of SiO_2–TiO_2 Janus particle or TiO_2 thin film on a glass surface also exhibits repelling power (Fig. 7). iii) Diffuse reflectance infrared Fourier transform spectroscopy (DRIFTS) analysis of the synthesized TiO_2 particles show no apparent peaks of organics at the 2960–2850 cm^{-1} C–H stretching region (Supporting Information Fig. S11).

4. Summary

Overall, the phenomena that we report are complex. The facts can be summarized as: i) methanol promotes the expansion motion with negative SiO_2 tracer particles due to higher reaction rate and more products produced, but causes some contractive motion with positive amidine-PS tracer particles because of the negative charge built up in the presence of the hole scavenger. ii) The existence of 1 M or higher concentration of TEMPO induces contractive motion near TiO_2 when SiO_2 is the tracer particle, either because TEMPO scavenges the radical products and reverses the radical concentration profile or because TEMPO scavenges electrons and makes the surface of TiO_2 more positive; that fact that this behavior is not observed with the positive amidine-PS tracer particle supports the second hypothesis. iii) A 0.5 mM 1:1 type electrolyte solution quenches the motion almost completely, suggesting an ionic diffusiophoretic mechanism or electrostatic interactions. iv) Diffusiophoresis model explains the trend of the movement of SiO_2 tracer particles, but fails to predict the movement of amidine-PS particles. Amidine-PS particles are predicted to move toward the TiO_2 while observations showed otherwise. This suggests an additional non-charge-related mechanism, possibly osmotic propulsion resulting from the diffusion of solutes. v) When a charge alteration occurs, either on TiO_2 or on nearby related substrates, the positively charged amidine-PS particles change their behavior in the opposite way to that of SiO_2 particles. Examples were seen with the addition of a hole scavenger (SiO_2 move farther away while amidine-PS sometimes pull in) or an electron scavenger (nearby SiO_2 pull in while amidine-PS consistently move out), or by changing the ζ-potential of the glass slide (SiO_2 move out as usual while amidine-PS pull in occasionally, discussed in Supporting Information). vi) Surface organic residues from the synthetic process is unlikely to be responsible for the firework phenomenon, for a) rinsing off the residues did not change the fireworks activity, b) noncontaminated TiO_2 films showed fireworks activity as well, and c) DRIFTS analysis showed no apparent organic contamination.

5. Conclusions

TiO_2 is a promising candidate for the next generation of self-propelled micro/nanomotors and microfluidic pumping systems with a number of advantages compared to the previously reported systems. It is highly active, inexpensive, clean and simple, requires little supply of fuels (e.g., alcohol), and produces no bubbles. It is easily controlled by UV light. With a little modification (e.g., dye sensitization[30]), visible light control could become possible. Reversible and repeatable ''microfireworks'' were observed around TiO_2 microparticles. The overall force is generally repulsive but can be modified by the addition of a radical scavenger or hole/electron scavenger. We believe the ''microfirework'' is a result of multiple mechanisms acting in concert: i) diffusiophoresis as a result of the differential diffusion of ionic products produced from TiO_2-catalyzed photoreactions. ii) Osmotic propulsion as a result of unequal solute molecule concentration on different sides of the tracer particle. The direction of osmotic propulsion is always toward the lower solute concentration region. iii) Surface charge interaction originating from UV-induced charge separation and redistribution on TiO_2.

Acknowledgements

We thank Dr. Darrell Velegol, Dr. Thomas Mallouk, and Dr. Vincent Crespi for helpful discussions. This project was funded by the National Science Foundation through the Center for Nanoscale Science (NSF-MRSEC, DMR-0820404). Support was also given by the NSF-supported Penn State University's National Nanotechnology Network (NNIN). Supporting Information is available online from Wiley InterScience or from the author. The Supporting Information includes several videos: *Video 1*: UV-induced movement of sub-micrometer TiO_2 particles in deionized water (movie was taken at 50× magnification); *Video 2*: UV-induced rotational movement of micrometer-sized TiO_2 particles in deionized water (movie was taken at 50× magnification); *Video 3*: SiO_2–TiO_2 Janus microparticles migrate toward the UV spot at the upper left corner upon long exposure (sped up 30× and taken at 20× magnification).

Received: January 11, 2010

[1] a) T. E. Mallouk, A. Sen, *Sci. Am.* **2009**, *300*, 72. b) J. Wang, K. M. Manesh, *Small* **2010**, *6*, 338. c) T. Mirkovic, N. S. Zacharia, G. D. Scholes, G. A. Ozin, *Small* **2010**, *6*, 159. d) Y. Hong, N. Chaturvedi, D. Velegol, A. Sen, *Phys. Chem. Chem. Phys.* **2010**, *12*, 1423.

[2] E. M. Purcell, *Am. J. Phys.* **1977**, *45*, 3.
[3] J. Happell, H. Brenner, in: *Low Reynolds Number Hydrodynamics*, Prentice Hall, Englewood Cliffs **1965**.
[4] a) E. M. Purcell, *Am. J. Phys.* **1977**, *45*, 3. b) A. Najafi, R. Golestanian, *Phys. Rev. E* **2004**, *69*, 062901. c) J. E. Avron, O. Kenneth, D. H. Oaknin, *New J. Phys.* **2005**, *7*, 234. d) R. Golestanian, T. B. Liverpool, A. Ajdari, *New J. Phys.* **2007**, *9*, 126. e) D. Fleishman, J. Klafter, M. Porto, M. Urbakh, *Nano Lett.* **2007**, *7*, 837. f) C. M. Pooley, G. P. Alexander, J. M. Yeomans, *Phys. Rev. Lett.* **2007**, *99*, 228103. g) R. Golestanian, A. Ajdari, *Phys. Rev. Lett.* **2008**, *100*, 038101. h) W. F. Paxton, S. Sundararajan, T. E. Mallouk, A. Sen, *Angew. Chem, Int. Ed.* **2006**, *45*, 5420. i) W. F. Paxton, A. Sen, T. E. Mallouk, *Chem. Eur. J.* **2005**, *11*, 6462. j) J. Wang, *ACS Nano* **2009**, *3*, 4. k) S. Sánchez, M. Pumera, *Chem. Asian J.* **2009**, *4*, 1402.
[5] U. M. Córdova-Figueroa, J. F. Brady, *Phys. Rev. Lett.* **2008**, *100*, 158303.
[6] J. Vicario, R. Eelkema, W. R. Browne, A. Meetsma, R. M. La Crois, B. L. Feringa, *Chem. Commun.* **2005**, 3936.
[7] D. Pantarotto, W. R. Browne, B. L. Feringa, *Chem. Commun.* **2008**, 1533.
[8] Y. Mei, G. Huang, A. A. Solovev, E. B. Ureña, I. Mönch, F. Ding, T. Reindl, R. K. Y. Fu, P. K. Chu, O. G. Schmidt, *Adv. Mater.* **2008**, *20*, 4085.
[9] a) W. F. Paxton, K. C. Kistler, C. C. Olmeda, A. Sen, S. K. S. Angelo, Y. Cao, T. E. Mallouk, P. E. Lammert, V. H. Crespi, *J. Am. Chem. Soc.* **2004**, *126*, 13424. b) W. F. Paxton, A. Sen, T. E. Mallouk, *Chem. Eur. J.* **2005**, *11*, 6462. c) W. F. Paxton, P. T. Baker, T. R. Kline, Y. Wang, T. E. Mallouk, A. Sen, *J. Am. Chem. Soc.* **2006**, *128*, 14881. d) T. R. Kline, W. F. Paxton, T. E. Mallouk, A. Sen, in: *Nanotechnology in Catalysis*, Vol. *3* (Eds: B. Zhou, S. Han, R. Raja, G. A. Somorjai), Springer, New York **2007**. e) Y. Wang, R. M. Hernandez, D. .J Bartlett, Jr, J. M. Bingham, T. R. Kline, A. Sen, T. E. Mallouk, *Langmuir* **2006**, *22*, 10451. f) R. Laocharoensuk, J. Burdick, J. Wang, *ACS Nano.* **2008**, *2*, 1069.
[10] U. K. Demirok, R. Laocharoensuk, K. M. Manesh, J. Wang, *Angew. Chem, Int. Ed.* **2008**, *47*, 9349.
[11] M. E. Ibele, Y. Wang, T. R. Kline, T. E. Mallouk, A. Sen, *J. Am. Chem. Soc.* **2007**, *129*, 7762.
[12] S. Fournier-Bidoz, A. C. Arsenault, I. Manners, G. A. Ozin, *Chem. Commun.* **2005**, 441.
[13] N. Mano, A. Heller, *J. Am. Chem. Soc.* **2005**, *127*, 11574.
[14] J. R. Howse, R. A. L. Jones, A. J. Ryan, T. Gough, R. Vafabakhsh, R. Golestanian, *Phys. Rev. Lett.* **2007**, *99*, 048102.
[15] A. Sen, M. E. Ibele, Y. Hong, D. Velegol, *Faraday Discuss.* **2009**, *143*, 15.
[16] M. Ibele, T. Mallouk, A. Sen, *Angew. Chem, Int. Ed.* **2009**, *48*, 3308.
[17] N. Chaturvedi, Y. Hong, A. Sen, D. Velegol, *Langmuir* **2010**, DOI: 10.1021/la904133a.
[18] S. Banerjee, J. Gopal, P. Muraleedharan, A. K. Tyagi, B. Raj, *Curr. Sci.* **2006**, *90*, 1378.
[19] S. Josset, N. Keller, M.-C. Lett, M. J. Ledoux, V. Keller, *Chem. Soc. Rev.* **2008**, *37*, 744.
[20] Y. M. Wang, S. W. Liu, Z. Xiu, X. B. Jiao, X. P. Cui, J. Pan, *Mater. Lett.* **2006**, *60*, 974.
[21] B. Liu, L. Wen, X. Zhao, *Mater. Chem. Phys.* **2008**, *112*, 35.
[22] V. N. Bogomolov, E. K. Kudinov, Y. A. Firsov, *Sov. Phys. Solid State* **1968**, *35*, 555.
[23] A. Kudo, Y. Miseki, *Chem. Soc. Rev.* **2009**, *38*, 253.
[24] M. L. Cerrada, C. Serrano, M. Sánchez-Chaves, M. Fernández-García, F. Fernández-Martín, A. de Andrés, R. J. Jiménez Riobóo, A. Kubacka, M. Ferrer, M. Fernández-García, *Adv. Funct. Mater.* **2008**, *18*, 1949.
[25] R. Golestanian, T. B. Liverpool, A. Ajdari, *Phys. Rev. Lett.* **2005**, *94*, 220801.
[26] a) J. L. Anderson, M. E. Lowell, D. C. Prieve, *J. Fluid Mech.* **1984**, *148*, 247. b) J. L. Anderson, *Annu. Rev. Fluid Mech.* **1989**, *21*, 61.
[27] Y. Gu, D. Li, *J. Colloid Interf. Sci.* **2000**, *226*, 328.
[28] K. Carlson, M. Hall, *Colloids Surf. A: Physicochem. Eng. Aspects* **2008**, *325*, 101.
[29] M. Jakob, H. Levanon, P. V. Kamat, *Nano Lett.* **2003**, *3*, 353.
[30] T. V. Nguyen, H. C. Lee, M. A. Khan, O. B. Yang, *Solar Energy* **2007**, *81*, 529.